Electronic Supplementary Material (ESI) for Nanoscale.
This journal is © The Royal Society of Chemistry 2024

Supporting Information

Iron Oxide Nanozymes Enhanced by Ascorbic Acid for Macrophage-Based Cancer Therapy

Zhongchao Yi, [a] Xiaoyue Yang, [a] Ying Liang, [b] and Sheng Tong *[a]

[a] Department of Biomedical Engineering, University of Kentucky, Lexington, Kentucky 40536, United States.

[b] New York Blood Center, New York, New York 10065, USA.

Supporting Figures

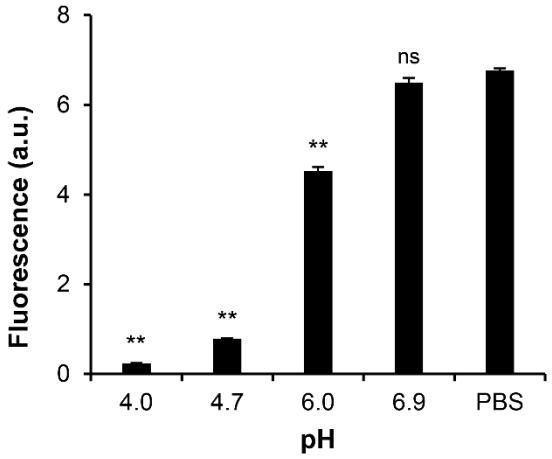

Figure S1. pH-dependency of Amplex Red. The Amplex Red generated in a peroxidase reaction was diluted 10 times by buffers of different pH levels. After dilution, fluorescence intensity was measured with a microplate reader. Data represents mean ± standard deviation (n = 3). **, $p < 0.01$ and ns, not significant vs. PBS.

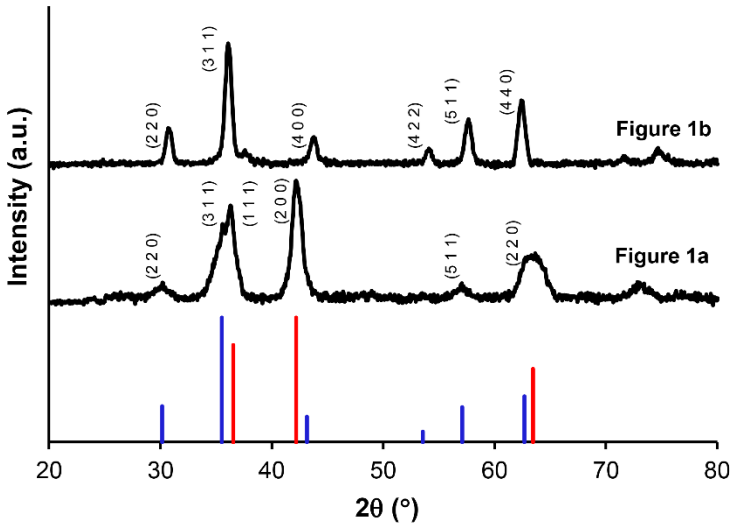

Figure S2. XRD patterns of nanocrystals shown in Figures 1a and 1b. Red and blue lines label the standard peaks of wüstite (PDF NO. 01-073-2144) and magnetite (PDF NO. 01-071-6336), respectively.

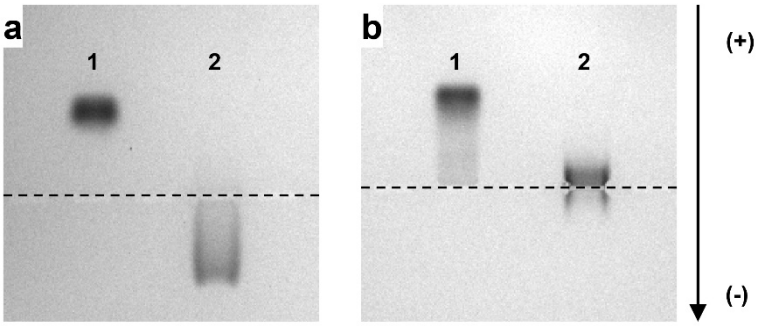

Figure S3. Gel electrophoresis of IONPs. WNPs and MNPs with and without TAT peptides were analyzed with gel electrophoresis in 0.6 % agarose gel. **a**. WNPs without TAT peptide (1) and with TAT peptide (2). **b**. MNPs without TAT peptide (1) and with TAT peptide (2). The “+” and “-” indicate anode and cathode in gel electrophoresis respectively.

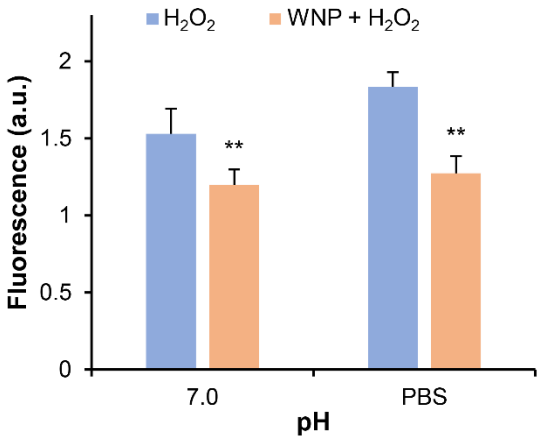

Figure S4. WNP catalysis at neutral pH. WNPs (20 μg Fe/mL) were added to a mixture of Amplex Red (50 μM), HRP (0.5 mU), and H_2O_2 (10 μM) in a 96-well plate. After 30 minutes of incubation, the fluorescence was measured with a microplate reader. Data represent mean ± standard deviation (n = 3). **, $p < 0.01$.

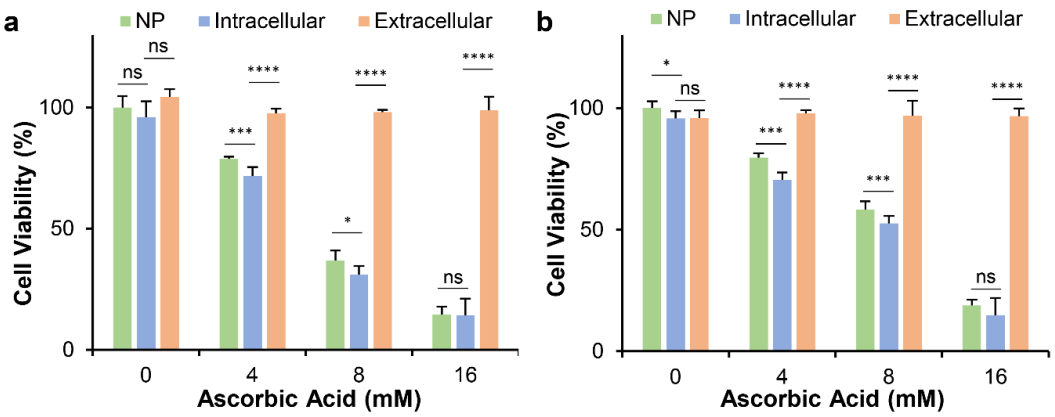

Figure S5. Cytotoxicity of ascorbic acid and MNPs. 4T1 (**a**) and RAW 264.7 cells (**b**) were treated with ascorbic acid alone or in the presence of intracellular or extracellular MNPs. Data represent mean ± standard deviation (n = 4).

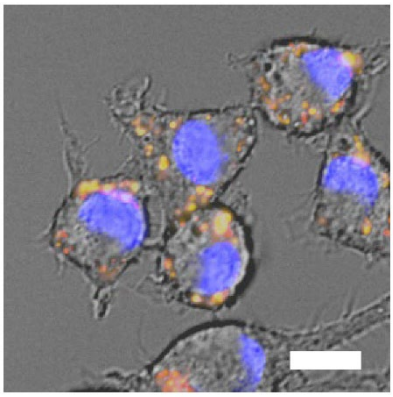

Figure S6. Intracellular distribution of IONPs. The brightfield and fluorescence images shown in Figure 3c were merged. Scale bar: 10 μm.

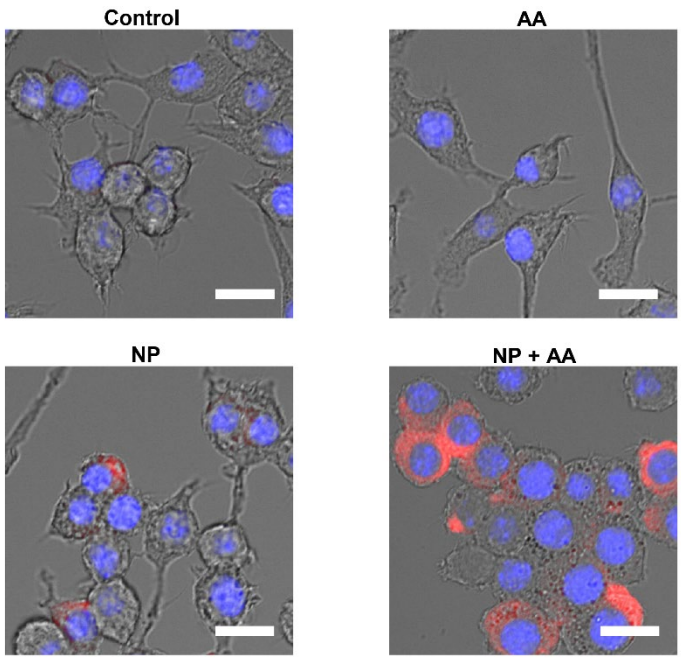

Figure S7. Expression of CD86 by RAW 264.7 cells. The fluorescence images shown in Figure 4d are merged with bright field images. Scale bar: 10 μm.

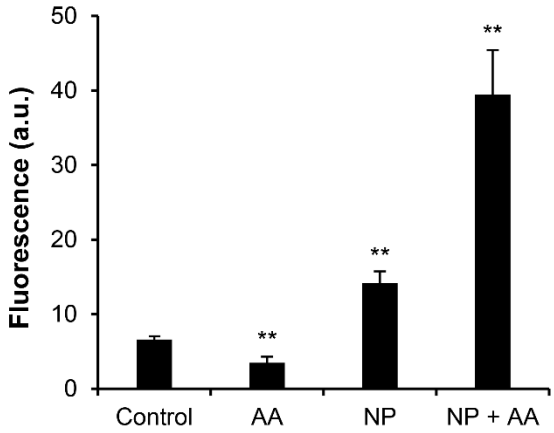

Figure S8. Expression of CD86 by RAW 264.7 cells. Fluorescence intensity was quantified using flow cytometry. Data represents mean ± standard deviation (n = 3). **, $p < 0.01$ vs. Control.

Supporting Tables

Table S1. Primers used for RT-qPCR gene expression analysis

Gene	Forward primer	Reverse primer
GAPDH	GCATCTTCTTGTGCAGTGCC	ACTGTGCCGTTGAATTTGCC
Arg-1	AACCAGCTCTGGGAATCTGC	TCCATCACCTTGCCAATCCC
CD206	GTCAGAACAGACTGCGTGGA	AGGGATCGCCTGTTTTCCAG
iNOS	GCCCAGCCAGCCCAAC	CTCAATGGCATGAGGCAGGA
CD86	ACGGACTTGAACAACCAGACT	CGTCTCCACGGAAACAGCAT
TNF-α	CAGTTCTATGGCCCAGACCC	TAGCAAATCGGCTGACGGTG
TGF-β	CTGCTGACCCCCACTGATAC	ATGTCATGGATGGTGCCCAG

Table S2. Characterization of DSPE-PEG-coated iron oxide nanoparticles.

	Core Size (nm)	Hydrodynamic Size (nm)	Polydispersity (%)
WNP	7.8 ± 0.8	22.0 ± 0.5	25.2
MNP	15.4 ± 1.3	30.9 ± 0.9	19.9

Table S3. Kinetics of IONP-mediated Fenton reaction

	V_{max} (nM S^{-1})	K_m (μM)
WNP	146.2	156.5
MNP	42.9	179.2
Ferumoxytol	35.9	395.6

The concentration of all IONPs was fixed at 20 μg Fe/mL.